CCC 2008 - Challenges for Civil Construction
Torres Marques et al. (Eds)

A MODEL TO SIMULATE THE CYCLIC AXIAL COMPRESSIVE BEHAVIOUR OF RC COLUMNS CONFINED WITH CFRP SHEETS

Rajendra K. Varma[*1], Joaquim A.O. Barros[*2], José Sena-Cruz[*3], Débora M. Ferreira[*4]

[*] ISISE, DEC, School of Engineering, University of Minho
Campus de Azurem, 4800-058 Guimarães, Portugal
e-mail: [1]rajendra@civil.uminho.pt, [2]barros@civil.uminho.pt, [3]jsena@civil.uminho.pt, [4]debora@ipb.pt
web page: www.civil.uminho.pt/composites

Keywords: Reinforced concrete columns, CFRP, concrete confinement, cyclic behaviour, fibrous model.

Summary: *In the present work a constitutive model to predict the cyclic axial compressive behavior of RC columns confined with CFRP is proposed. This model was implemented in a FEM-based computer program, able to simulate the material nonlinear behavior of reinforced concrete frame structures. The performance of the developed model is assessed using results obtained from experimental tests.*

1 INTRODUCTION

The use of Carbon Fiber Reinforced Polymer (CFRP) materials has increased significantly in the last decade. In fact, fully or partially wrapping concrete circular columns with wet lay-up CFRP sheets can significantly increase the load carrying and energy absorption capacities of these elements. The effectiveness of this CFRP-based confinement strategy depends on several parameters such as: concrete strength, CFRP percentage, geometric confinement arrangement, column aspect ratio, disposition and percentage of existing steel reinforcement. Some properties of CFRP sheets like low weight, high strength and easy installation make these composites highly suitable for concrete confinement.

Several researchers [1-6] have contributed to understand the role of CFRP sheets as a material for the concrete confinement. Most of the experimental studies have been carried out to acquire enough and reliable data that can be used to propose analytical models for the simulation of the behavior of FRP-based concrete columns.

Typically, the studies have been limited to monotonic compressive loading, except few ones [7,8,12], which have explored the influence of the cyclic loading on the behavior of FRP-based confined concrete elements. Introducing some empirical adjustments to the stress-strain model proposed by Mander *et al.* [10] for steel confined concrete columns, some researchers [1,9] have assumed constant confining pressure exerted by CFRP. It should be noted, however, that this assumption is not appropriate because FRP has a linear elastic behavior up to failure. According to the knowledge of the authors of the present work, there is no constitutive model able of reproducing with enough accuracy the behavior of CFRP-based fully and partially confined RC columns subjected to cyclic compressive loading.

In the present work, a constitutive model for CFRP-based confined circular concrete columns subjected to monotonic and cyclic loadings is proposed. The constitutive model was implemented into FEMIX computer program, a FEM-based software for the nonlinear analysis of concrete structures. The performance of the developed constitutive model was appraised taking the experimental results from the tests carried out with RC column elements confined with CFRP sheets, and subjected to monotonic and cyclic axial compressive loading.

2 EXPERIMENTAL PROGRAM

The experimental program consists of monotonic and cyclic axial compression tests and is composed by three groups (G1, G2 and G3) of concrete cylinders of 200 mm diameter and 600 mm high. A total of 54 concrete cylinders were tested to appraise the effectiveness of full and distinct partial confinement CFRP arrangements. The experimental program aimed to study the effect of the following parameters on concrete confinement effectiveness: concrete strength class, stiffness and percentage of the wet lay-up CFRP sheet, width of the CFRP strip, and number of CFRP layers composing each strip. Each specimen is designated as W*i*S*j*L*k*F*l*_c/m, where W*i* represents the strip width, S*j* is the number of strips along the depth of a cylinder, L*k* represents the number of CFRP layers of each strip, and F*l* indicates the steel bar diameter. The c/m character is attributed to distinguish monotonic and cyclic tests. Fig. 1 and Tables 1-4 include the characteristics of concrete cylinders of the groups of tests composing the experimental program. In Tables 1-4, $f_{co,UPC}$ and $\varepsilon_{co,UPC}$ (see Fig. 3) are the compressive strength of unconfined plain concrete (UPC) specimen and its corresponding axial strain, respectively. Similarly, f_{cu} and ε_{cu} are the ultimate concrete compressive strength of CFRP confined concrete specimen and its corresponding axial strain, respectively. The parameter t_f is the thickness of the CFRP sheet, and ρ_f is the CFRP volumetric ratio given by:

$$\rho_f = 4 \cdot \frac{W \cdot L \cdot S \cdot t_f}{D \cdot H} \tag{1}$$

where *D* and *H* are the diameter and height of a specimen, respectively. The numerical values of the *W*, *L* and *S* can be derived from the specimen name as described above. CFRP confined and UPC cylinders of each series were prepared from the same concrete batch [13]. Two cylinders were tested for each confinement arrangement, as well as for UPC. More details can be found elsewhere [6,13].

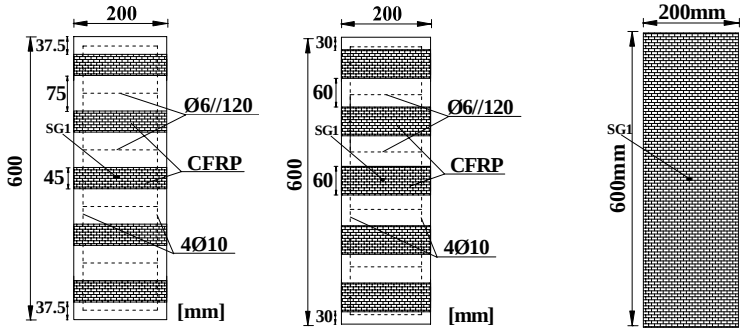

Figure 1: Confinement arrangements of the tested specimens: (a) W45 series, (b) W60 series and (c) W600 series.

2.1 Material Properties

Two types of CFRP sheets were used in the experimental program, with the trade names of CF120 (200 g/m^2 of fibres) and CF130 (300 g/m^2 of fibres). The mechanical properties of the sheets were determined from experimental tests on five samples for each type of sheet. The tests were conducted according to ISO recommendations [14]. The values indicated in Table 5 for the tested properties are the average results of five samples.

Table 1: Mechanical properties of specimens.

Group name	$f_{co,UPC}$ [MPa]	$\varepsilon_{co,UPC}$ [-]
G1	13.87	0.0027
G2	30.31	0.0031
G3	26.47	0.0030

Table 2: Characteristics of the G1 group of tests.

Specimen name	t_f [mm]	ρ_f	$\varepsilon_{cu}/\varepsilon_{co,UPC}$	$f_{cu}/f_{co,UPC}$
W45S6L3F8_m	0.113	0.0031	5.82	1.99
W45S6L5F8_m		0.0051	9.09	2.56
W60S6L3F8_m		0.0041	6.36	2.48
W60S6L5F8_m		0.0068	10.30	3.14
W600S1L3F8_m		0.0068	9.39	3.45
W600S1L5F8_m		0.0113	12.12	4.47
W45S6L3F8_m	0.176	0.0048	10.00	2.60
W45S6L5F8_m		0.0079	13.94	3.30
W60S6L3F8_m		0.0063	11.18	3.33
W60S6L5F8_m		0.0106	17.58	4.68
W600S1L3F8_m		0.0106	10.00	3.76
W600S1L5F8_m		0.0176	14.85	5.42
W45S5L3F10_m	0.113	0.0025	6.09	1.95
W45S5L5F10_m		0.0042	9.60	2.37
W60S5L3F10_m		0.0034	7.91	2.37
W60S5L5F10_m		0.0057	12.27	3.16
W600S1L3F10_m		0.0068	8.98	3.38
W600S1L5F10_m		0.0113	10.41	4.06
W45S5L3F10_m	0.176	0.0040	8.60	2.23
W45S5L5F10_m		0.0066	12.12	2.76
W60S5L3F10_m		0.0053	9.78	2.66
W60S5L5F10_m		0.0088	12.22	3.34
W600S1L3F10_m		0.0106	12.87	4.52
W600S1L5F10_m		0.0176	14.55	5.42

Table 3: Characteristics of the G2 group of tests.

Specimen name	t_f [mm]	ρ_f	$\varepsilon_{cu}/\varepsilon_{co,UPC}$	$f_{cu}/f_{co,UPC}$
W45S6L3F8_m	0.113	0.0031	3.07	1.48
W45S6L5F8_m		0.0051	4.63	1.83
W60S6L3F8_m		0.0041	4.57	1.79
W60S6L5F8_m		0.0068	5.97	2.21
W600S1L3F8_m		0.0068	6.03	2.35
W600S1L5F8_m		0.0113	4.67	2.36
W45S6L3F8_m	0.176	0.0048	4.40	1.74
W45S6L5F8_m		0.0079	6.17	2.00
W60S6L3F8_m		0.0063	6.17	2.10
W60S6L5F8_m		0.0106	7.50	2.57
W600S1L3F8_m		0.0106	5.60	3.09
W600S1L5F8_m		0.0176	4.03	3.83
W45S5L3F10_m	0.113	0.0025	2.28	1.43
W45S5L5F10_m		0.0042	2.81	1.62
W60S5L3F10_m		0.0034	2.68	1.58
W60S5L5F10_m		0.0057	3.50	1.69
W600S1L3F10_m		0.0068	4.17	2.36
W600S1L5F10_m		0.0113	2.66	3.31
W45S5L3F10_m	0.176	0.0040	3.18	1.52
W45S5L5F10_m		0.0066	4.13	1.79
W60S5L3F10_m		0.0053	3.50	1.85
W60S5L5F10_m		0.0088	5.03	2.12
W600S1L3F10_m		0.0106	2.91	3.17
W600S1L5F10_m		0.0176	3.05	3.67

Table 4: Characteristics of the G3 group of tests.

Specimen name	t_f [mm]	ρ_f	$\varepsilon_{cu}/\varepsilon_{co,UPC}$	$f_{cu}/f_{co,UPC}$
W45S6L3F8_m	0.113	0.0031	6.00	1.49
W45S6L5F8_m[b]		0.0051	8.00	1.97
W60S6L3F8_m		0.0041	6.33	1.89
W60S6L5F8_m		0.0068	6.67	2.42
W600S1L3F8_m		0.0068	8.33	2.11
W45S6L3F8_c		0.0031	5.00	1.62
W45S6L5F8_c		0.0051	8.33	1.85
W60S6L3F8_c		0.0041	6.33	1.78
W60S6L5F8_c[b]		0.0068	9.33	2.03
W600S1L3F8_c		0.0068	4.67	2.69

[b] Used for simulation.

Table 5: CFRP properties (average of five tests)

CFRP Sheets	Thickness [mm]	Tensile strength [MPa]	Ultimate strain [%]	Elasticity modulus [GPa]
CF120	0.113	3535	1.52	232
CF130	0.176	3070	1.33	230

2.2 Test procedure

Three Linear Variable Displacement Transducers (LVDTs) were placed at 120° from each other around the cylindrical specimen to measure the displacements between the steel load plates of the equipment (Fig. 2). From the values recorded in these three LVDTs the specimen axial displacement is determined, from which the axial strain is calculated dividing this value by the specimen initial height. This monitoring arrangement avoids that the deformation of the equipment has been added to the values recorded by the LVDTs.

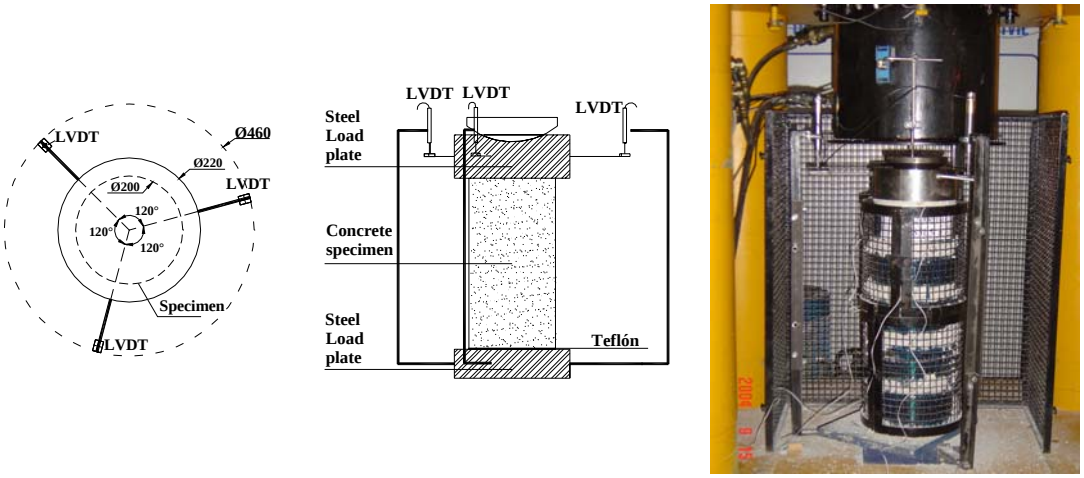

Figure 2: Position of the LVDTs and test apparatus.

2.3 Experimental results from other researchers

For the purpose of collecting data for the definition of the parameters participating in the constitutive model developed within the ambit of the present work, data from other researchers [16-20] was also used.

3 CONSTITUTIVE MODEL FOR CFRP CONFINED CONCRETE ELEMENTS

The developed constitutive model is described in following two sections, one dedicated to the compression envelope curve (the monotonic loading curve for compression) and the other for the cyclic hysteretic branches.

3.1 Compression envelope curve

The envelope curve for compression is based on Lam and Teng model [5]. The stress-strain relationship of the envelope curve (see Fig. 3), f_c-ε_c, can be described as follows:

For $0 \le \varepsilon_c \le \varepsilon_{ct}$

$$f_c = E_c \varepsilon_c - \frac{(E_c - E_{c2})^2}{4 f_0} (\varepsilon_c)^2 \tag{2}$$

For $\varepsilon_{ct} < \varepsilon_c \le \varepsilon_{cu}$

$$f_c = f_0 + E_{c2} \varepsilon_c \tag{3}$$

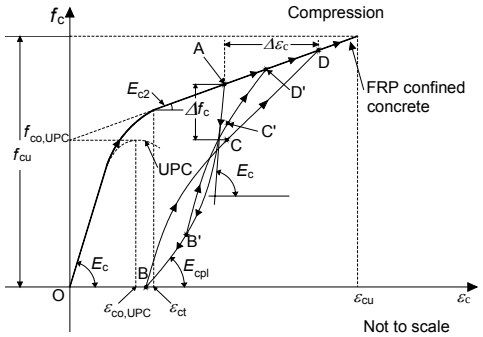

Figure 3: Schematic representation of the FRP-confined concrete constitutive model

where $f_0 = f_{co,UPC}$; E_c is the concrete initial Young's modulus calculated using CEB-FIB Model Code 1990 [21] for UPC; ε_{ct} is the strain at the transition between the domain of the equation (2) and (3), defined as:

$$\varepsilon_{ct} = \frac{2f_0}{(E_c - E_{c2})} \tag{4}$$

where E_{c2} is the concrete tangential Young's modulus described by:

$$E_{c2} = \frac{f_{cu} - f_0}{\varepsilon_{cu}} \tag{5}$$

For partially confined concrete, f_{cu} and ε_{cu} are described by the Fig. 4(a-b) as:

$$f_{cu} = (214\rho_f + 1.069)f_{co} \text{ for } 0.0025 \le \rho_f \le 0.0106 \tag{6}$$

$$\varepsilon_{cu} = (907.6\rho_f + 2.296)\varepsilon_{co} \text{ for } 0.0025 \le \rho_f \le 0.0106$$

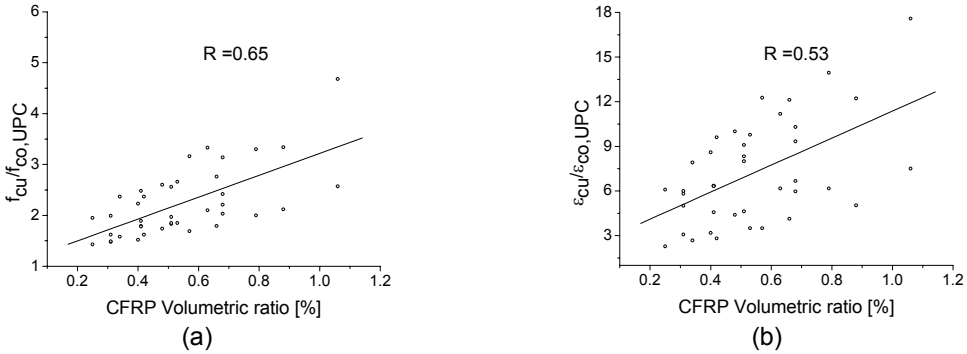

Figure 4: Diagram used for interpolation of (a) f_{cu} and (b) ε_{cu} for partially confined specimen.

Similarly for completely confined concrete, data was acquired from other researchers [16-20] (not presented here); the equations are illustrated by Fig. 5(a-b) as:

$$f_{cu} = (72.99\rho_f + 1.3389) f_{co,UPC} \text{ for } 0.0016 \le \rho_f \le 0.0272 \quad (7)$$

$$\varepsilon_{cu} = (535.91\rho_f + 1.6049) \varepsilon_{co,UPC} \text{ for } 0.0016 \le \rho_f \le 0.0272$$

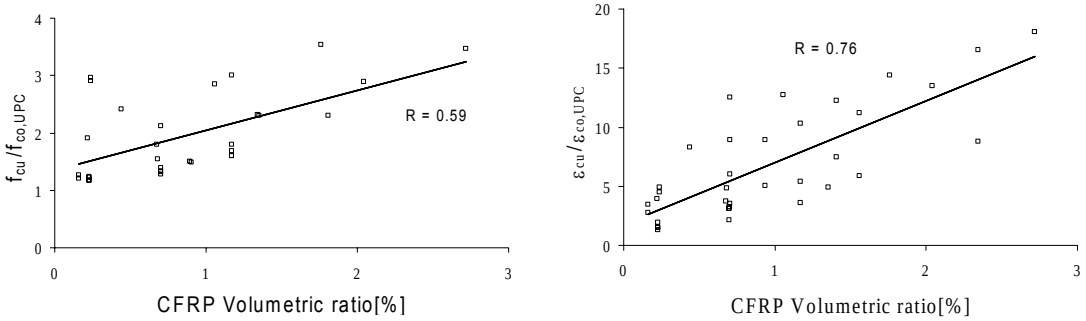

(a) (b)

Figure 5: Diagram used for interpolation of (a) f_{cu} and (b) ε_{cu} for completely confined specimen.

3.2 Cyclic hysteretic branches

The complete cyclic hysteretic scheme for compression can be completely described by four rules and their modified form. The cyclic hysteretic branches described here include nonlinear unloading/reloading, arbitrary cyclic loading and, stiffness degradation resulting from cyclic loading. The shapes of all possible complete or partial cyclic branches are predicted by transition curves. The transition curves starts from an already well-known starting point (ε_{ca}, f_{ca}) (a subscript *a* is used to designate starting point) with slope (E_{ca}) that needs to be evaluated, and ends at a target point (ε_{cb}, f_{cb}) (a subscript *b* is used to designate ending point), whose coordinates, as well as the slope at this point (E_{cb}) need to be calculated. The transition curve is represented the following equation:

$$f_c = f_{ca} + (\varepsilon_c - \varepsilon_{ca})[E_{ca} + A_c \left|\varepsilon_c - \varepsilon_{ca}\right|^{R_c}] \quad (8)$$

where R_c is the parameter governing curvature and A_c is an internal parameter given by:

$$R_c = \frac{E_{cb} - E_{c\sec}}{E_{c\sec} - E_{ca}},\ A_c = \frac{E_{c\sec} - E_{ca}}{\left|\varepsilon_{cb} - \varepsilon_{ca}\right|^{R_c}} \text{ and } E_{\text{csec}} = \frac{f_{cb} - f_{ca}}{\varepsilon_{cb} - \varepsilon_{ca}} \quad (9)$$

where E_{csec} represents the secant modulus.

The proposed compressive hysteretic scheme shown in Fig. 3, with all the possible cases, can be broadly categorized as: (i) complete unloading (AB); (ii) partial unloading (AB'); (iii) complete reloading (BCD); and, (iv) partial reloading (B'C'D').

Complete unloading here refers to unloading from envelope curve until zero stress; similarly, complete reloading refers to reloading until envelope curve and; partial unloading/reloading refers to all the other possible unloading/reloading which does not fall into the above categories. Unloading from point A (ε_{cun}, f_{cun}) with reversal slope E_{cun} (= E_c, see Fig. 3), will target, point B (ε_{cpl}, 0) with target slope E_{cpl}; whose characteristic parameters can be found as follows:

$$E_{\text{cpl}} = 0.1 E_c \exp\left(-2\left|\frac{\varepsilon_{cun}}{\varepsilon_{cu}}\right|\right) \quad (10)$$

$$\varepsilon_{cpl} = \varepsilon_{cun} - \frac{f_{cun}}{E_{c\,\sec}}$$

while E_{csec} can be described as:

$$E_{csec} = 0.38 E_c \left(\frac{\varepsilon_c}{\varepsilon_{cu}} \right)^{-0.28} \tag{11}$$

The transition curve equation (8) is used to join the initial point A and the target point B.

A reversal from any point in between A and B, will initiate the starting of a reloading curve. The complete reloading curve is described by three point and two connecting transition curves; an initial point B, an intermediate point C and a target point D. The first transition curve connects the point B (ε_{cpl}, 0) with starting slope E_c, to an intermediate point C (ε_{cun}, f_{cnew}) with slope E_{cnew}. Similarly, the second transition curve connects the intermediate point C (ε_{cun}, f_{cnew}) with slope E_{cnew}, to the return point D (ε_{cre}, f_{cre}) with target slope E_{cre}. The parameters required for complete reloading are derived as follows:

$$f_{cnew} = f_{cun} - \Delta f_c \tag{12}$$

$$E_{cnew} = \frac{f_{cnew}}{\varepsilon_{cun} - \varepsilon_{cpl}} \tag{13}$$

$$\varepsilon_{cre} = \varepsilon_{cun} + \Delta\varepsilon_c \tag{14}$$

$$E_{cre} = E_c \left(\varepsilon_{cre} \right) \tag{15}$$

$$f_{cre} = f_c \left(\varepsilon_{cre} \right) \tag{16}$$

$$\Delta f_c = 0.09 f_{cun} \sqrt{\left| \frac{\varepsilon_{cun}}{\varepsilon_{cu}} \right|} \tag{17}$$

Above Eqns. (12-17) are described in detail elsewhere [11]. According to Barros et al. [12] the strain shift $\Delta\varepsilon_c$ can be obtained from:

$$\Delta\varepsilon_c = 0.1992 \ \ \varepsilon_{cun} \tag{18}$$

For reloading followed by partial unloading, a modified returning point is defined which is calculated from the modified eqns (12-16) using linear interpolation, as follows:

$$f_{cnew^*} = f_{cun} - \Delta f_c \ \frac{\varepsilon_{cun} - \varepsilon_{cro}}{\varepsilon_{cun} - \varepsilon_{cpl}} \tag{19}$$

$$E_{cnew^*} = \frac{f_{cnew^*} - f_{cro}}{\varepsilon_{cun} - \varepsilon_{cro}} \tag{20}$$

$$\varepsilon_{cre^*} = \varepsilon_{cun} + \Delta\varepsilon_c \frac{\varepsilon_{cun} - \varepsilon_{cro}}{\varepsilon_{cun} - \varepsilon_{cpl}} \tag{21}$$

$$E_{cre^*} = E_c\left(\varepsilon_{cre^*}\right) \tag{22}$$

$$f_{cre^*} = f_c\left(\varepsilon_{cre^*}\right) \tag{23}$$

where (ε_{cro}, f_{cro}) refers to reversal point B' (see Fig. 3) located on unloading curve, C' (ε_{cun^*}, f_{cnew^*}) and D'(ε_{cre^*}, f_{cre^*}) designate the modified coordinates found by the linear interpolation, as reported by Chang and Mander [11]. Chang and Mander stated that similar linear interpolation can be used for partial reloading or arbitrary unloading/reloading.

4 NUMERICAL SIMULATIONS

4.1 Introduction

A fibrous model with cyclic constitutive laws for CFRP confined concrete and steel was implemented into FEMIX computer program, which is based on the finite element method (FEM). This model is capable of analyzing the nonlinear cyclic behavior of three-dimensional reinforced concrete (RC) frames. Each element is discretized in fibers along its longitudinal direction. The behavior of each fiber can be independent at material level, while the kinematic relation integrates them at structural level. A constitutive law is applied to every fiber at material level, according to the material characteristic and, a response is generated from each fiber. The collective response of the fibers produces the response at structural level.

By comparing the stress-strain relationships recorded in the experimental tests performed by Debora [13] with those obtained from the simulations of the tested columns, the performance of the implemented model to predict the response of confined cylindrical columns was assessed. In the present numerical simulations, all the columns were discretized with three FE isoparametric elements of three nodes each, and two Gauss integration points per element were considered for the evaluation of the stiffness matrix and internal forces. The concrete area of the cross section was discretized in forty-eight quadrilaterals elements of eight nodes, while four quadrilaterals elements of four nodes were used to discretize the cross section of the steel bars. An integration scheme of 2×2 Gauss integration points was used for the calculation of the stiffness matrix and internal forces of every elements of the specimen cross section. The steel bars were assumed as being perfectly bonded to the surrounding concrete. A detailed description of the material constitutive law used to simulate the steel cyclic behavior can be found in elsewhere [11].

4.2 Model appraisal

4.2.1 Monotonic loading

The characteristic of the material parameters for the material constitutive laws defining the CFRP confined concrete are included in Tables 1 and 4. To define the cyclic model for the steel bars, the values indicated in Table 6 were used. In this table, f_{sy}, f_{sh} and f_{su} represent the steel yield stress, the hardening stress and the ultimate tensile stress, respectively, while ε_{sh} and ε_{su} represent the steel strain corresponding to f_{sh} and f_{su}, respectively. Parameters E_s and E_{sh} represent the elasticity modulus and tangent modulus at hardening strain, respectively.

Simulation of tests conducted by other researchers was also performed [5]. The corresponding data for the simulations is presented in Table 7.

Table 6: Mechanical properties of the steel bars.

Specimen	E_s [MPa]	f_{sy} [MPa]	ε_{sh} [-]	f_{sh} [MPa]	ε_{su} [-]	f_{su} [MPa]	E_{sh} [MPa]
W45S6L5F8_m	200000	328	0.0075	517	0.110	540	6400
W60S6L5F8_c	216900	328	0.0075	517	0.110	540	6400

Fig. 6 shows the typical simulation performance obtained for the monotonic loading tests. It can be concluded that the constitutive model simulates with good accuracy the stress-strain responses registered in CFRP-based confined concrete cylinders. However, in the phase governed by the CFRP characteristics ($\varepsilon_{ct} < \varepsilon_c \leq \varepsilon_{cu}$) some experimental responses showed a slight curvature on the stress-strain relationship that was not well captured by the present model, since it assumes that the stress is linearly dependent on the strain.

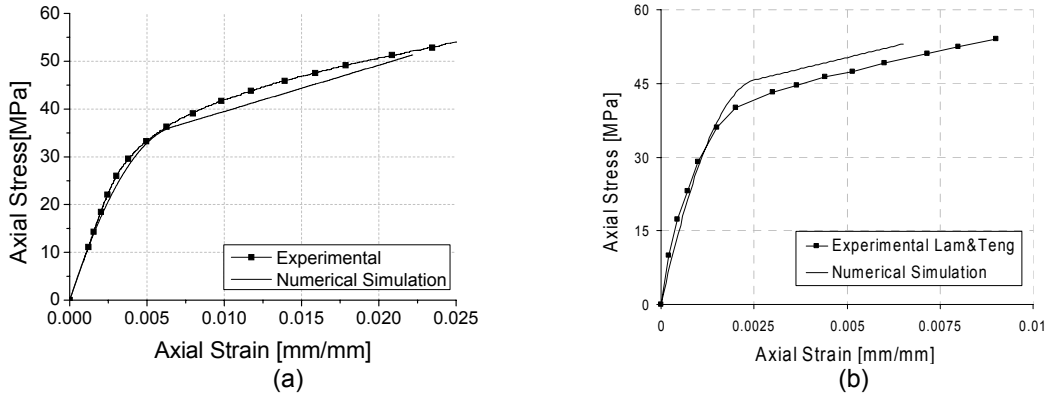

Figure 6: Experimental results and numerical simulations under monotonic loading: (a) specimen W45S6L5F8_m; (b) specimen from Lam and Teng [5].

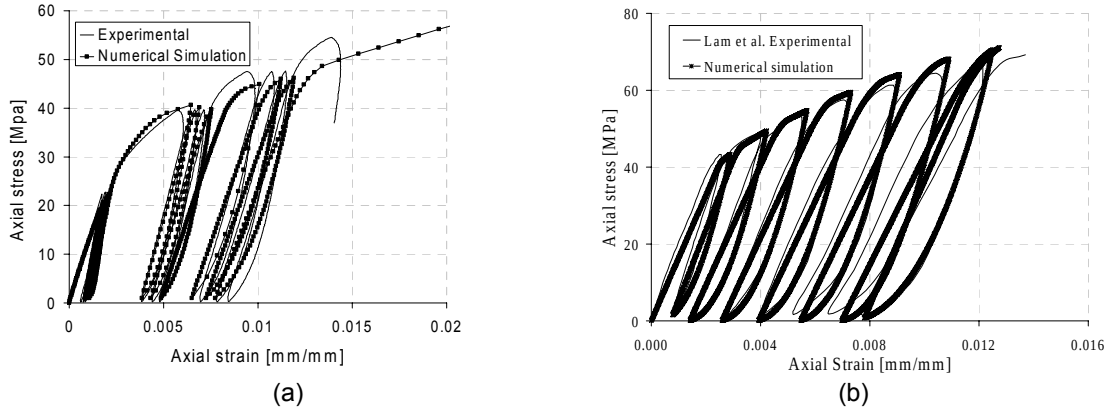

Figure 7: Experimental results and numerical simulations under cyclic loading: (a) specimen W60S6L5F8_c; (b) specimen from Lam et al. [8].

4.2.2 Hysteretic load simulations

Fig. 7a represents the typical performance of the developed cyclic model when applied to the simulations of the tests carried out by Ferreira [13] and Lam et al. [8]. The values of the model parameters used for the simulation of W60S6L5F8_c specimen are included in Table 1, 4 and 6 (the *b* superscript in Table 4 indicates the simulated specimen). Simulation of cyclic loading tests conducted by other researchers [8] was also performed. The experimental and the numerical stress-strain curves are represented in Fig. 7b. The corresponding data for the simulation is presented in Table 7. From Fig. 7 in can be concluded that the developed model is able to simulate with acceptable accuracy the stress-strain response registered in CFRP-based confined concrete columns subjected to cyclic loading. The stress and stiffness degradation due to the imposed cycles, during the axial deformation of the specimen, was well captured.

Table 7: Characteristic parameters used for simulation.

Specimen	ρ_f [%]	f_{co} [MPa]	ε_{co} [-]
Lam and Teng [5]	0.0043	41.1	0.00256
Lam et al. [8]	0.0087	38.9	0.00250

5 CONCLUSIONS

In the present work a model to predict the cyclic axial compressive behavior of RC columns confined with CFRP was proposed. The monotonic phase of the model is based on the proposal by Lam and Teng. On the other hand, the cyclic phase is based on the proposal by Chang and Mander. Some adjustments were done in the formulations of both phases, in order to take into account the confinement characteristics provided by CFRP materials. The adjustments were based on results obtained from an extensive experimental program with CFRP-based confined RC column specimens of circular cross section.

The model was implemented into the FEMIX computer program, which is based on the finite element method (FEM). To evidence the possibilities and deficiencies of the developed model, the results of some of the numerical simulations are presented and analyzed. The model was able of predicting with acceptable accuracy the stress-strain response of CFRP-based confined concrete columns of circular cross section, for both monotonic and cyclic loadings. However, the proposed model can be improved in terms of envelope curve, by considering a slightly curved behaviour instead of linear behavior for the phase governed by the influence of the CFRP.

ACKNOWLEDGEMENTS

The first author acknowledges the support provided by the grant within the ambit of the research program PABERPRO supported by Program POCI 2010 – IDEIA, Project nº 13-05-04-FDR-00007, contract reference ADI/2007/V4.1/0049. The authors wish to acknowledge the materials generously supplied by S&P® and degussa® Portugal.

REFERENCES

[1] H. Saadatmanesh, M.R. Ehsani, and M.W. Li, “Strength and ductility of concrete columns externally reinforced with fiber composite straps”, ACI Struct. J., 91(July–Aug.), 434–447 (1994).

[2] A. Nanni and M.N. Bradford, “FRP jacketed concrete under uniaxial compression”, Constr. and Build. Mat., 9(2), 115–124 (1995)

[3] F. Picher, P. Rochette, P. Labossie`re, “Confinement of concrete cylinders with CFRP”, Proc., First Int. Conf. on Compos. Infrastructures, Tucson, Ariz., 829–841 (1996)

[4] M.R. Spolelstra, G. Monti, “FRP-Confined Concrete Model”, Journal of Composites for Construction, ASCE; 3(3):144-150 (1999)
[5] L. Lam, and J.G. Teng, “Design-oriented stress-strain model for FRP-confined concrete”, J. Construction and building materials, Elsevier, vol. 17, 471-489 (2003)
[6] J.A.O Barros, D.R.S.M. Ferreira, “Assessing the efficiency of CFRP discrete confinement systems for concrete column elements”, in press, Journal of Composites for Construction (2007).
[7] Y. Shao, Z. Zhu, A. Mirmiran, “Cyclic Modeling of FRP-Confined Concrete with Improved Ductility”, Cement & Concrete Composites, Elsevier, 28(10), 959-968 (2006)
[8] L Lam, J.G. Teng, C.H. Cheung, and Y. Xiao, “FRP-confined concrete under cyclic axial compression”, Cement & Concrete Composites, 28, 949-958 (2006)
[9] F. Seible, A. Burgueno, M.G. Abdallah, R. Nuismer, “Advanced composites carbon shell system for bridge columns under seismic loads”, In: Proceedings, National Seismic Conference on Bridges and Highways: San Diego, USA (1995)
[10] J.B. Mander, M.J.N. Priestley, R. Park, “Theoretical stress–strain model for confined concrete”, J Struct Eng, ASCE; 114(8):1804 –26 (1988)
[11] G.A. Chang and J.B. Mander, “Seismic energy based fatigue damage analysis of bridge columns: Part I-Evaluation of seismic capacity”, Tech. Report NCEER-94-0006 (1994)
[12] J.A.O. Barros, D.R.S.M. Ferreira, R.K. Varma, “CFRP confined reinforced concrete elements submitted to direct cyclic compressive loading”, Special Publication “Seismic Strengthening of Concrete Buildings using FRP Composites” Paper SP-06 (2007)
[13] D.R.S.M. Ferreira, “CFRP-based confinement of circular concrete column elements – experimental and analytical research”, PhD thesis, University of Minho, 2007. (in Portuguese).
[14] ISO TC 71/SC 6 Non-conventional reinforcement of concrete-test methods-part 2: Fiber reinforced polymer (FRP) sheets, International standard (2003)
[15] J. A. O. Barros and D. R. S. M. Ferreira, “Partial versus full wrapping confinement systems for concrete columns”, International Conference on Concrete Repair, Rehabilitation and Retrofitting, South Africa, 1123-1129 (2005)
[16] S. Matthys, L. Taerwe, K. Audenaert, “Tests on axially loaded concrete columns confined by fiber reinforced polymer sheet wrapping”. In: Dolan C.W., Rizkalla S.H., and Nanni S.H., editors, Proceedings of the Fourth International Symposium on Fiber Reinforced Polymer Reinforcement for Reinforced Concrete Structures, SP-188, Farmington, Michigan, USA: American Concrete Institute:217–229 (1999)
[17] A. Mirmiran and M. Shahawy, “Behavior of concrete columns confined by fiber composites”, J. Struct. Engrg., ASCE, 123(5), 583–590 (1997)
[18] S. Pessiki, K.A. Harries, J.T. Kestner, R. Sause, J.M. Ricles “Axial behavior of reinforced concrete columns confined with FRP jackets”, J Compos Constr ASCE;5(4):237 –45 (2001)
[19] T.C. Rousakis, A.I. Karabinis, P.D. Kiousis, “FRP-confined concrete members: Axial compression experiments and plasticity modelling”, Article in press Engineering Structures, doi:10.1016/j.engstruct.2006.08.006
[20] L. De Lorenzis, F. Micelli, A. La Tegola, “Influence of specimen size and resin type on the behavior of FRP-confined concrete cylinders”, In: Shenoi R.A., Moy S.S.J., Hollaway L.C., editors, Advanced Polymer Composites for Structural Applications in Construction, Proceedings of the First International Conference, London, UK: Thomas Telford,:231–239 (2002)
[21] CEB-FIP. “Model code”, Thomas Telford, p.437 (1990)